Journal of Mines, Metals and Fuels, *71(10): 1474-1482; 2023. DOI: 10.18311/jmmf/2023/35793*

Print ISSN : 0022-2755

Journal of Mines, Metals and Fuels

Contents available at: *www.informaticsjournals.com/index.php/jmmf*

A Numerical Analysis of Reiner-Philippoff Fluid Flow on a Stretching Sheet with the Effect of Ohmic, Viscous Dissipation and First Order Slip

Y. S. Kalyan Chakravarthy*, S. Ram Prasad and S. H C. V. Subba Bhatta

Department of Mathematics, M. S. Ramaiah Institute of Technology, Bangalore – 560054, India; yskchakri@gmail.com

Abstract

In this study, by considering the effects of joule heating and viscous dissipation, we analyzed the Reiner-Philippoff fluid flow along a stretching sheet. Velocity slip of first order is taken into account. Using the Shooting method, the transformed governing equations are numerically solved. Graphical analysis is used to examine how new parameters affect the fields of temperature and velocity. The obtained results are compared to the results that have been published and are found to be in strong agreement. Examples of this kind of flow on a stretching sheet include the extrusion of polymers, liquid coatings, and other procedures.

Keywords: *Joule Heating, Reiner-Philippoff Fluid, Stretching Sheet*

1.0 Introduction

A non-Newtonian fluid is one that changes nonlinearly under fluid stress and displays nonlinear viscosity. The importance of non-Newtonian fluids in industry and engineering has amorousness many researchers. In addition, non-Newtonian behavior finds application in the mining sector, where muds and slurries are frequently handled, as well as in biomedical flows and lubrication. Additionally, non-Newtonian fluids are used to raise the calibre of printing processes. Research indicates that natural thickeners for printer ink can be derived from thixotropic or shear thinning fluids, like sodium alginate, modified starch, and cellulose derivatives. The viscosity and flow characteristics of the ink are enhanced by these non-Newtonian fluids, making printing more clear. A Reiner-Philippoff fluid model, one of the most significant non-Newtonian fluid models, which displays both non-Newtonian and Newtonian behaviour as a result of variable fluid shear rates. The explanation about the Reiner-Philippoff fluid model was initially developed by Kapur and Gupta[1]. Numerical analysis is used to examine the flow of a classical non-Newtonian fluid, the Reiner-Philippoff fluid, across a stretching sheet when nanoparticles are present. The nonlinear stress-deformation behaviour for the Reiner-Philippoff fluid as well as Brownian motion and nanoparticle-induced thermophoresis effects are incorporated into the mathematical model by Adeel Ahmad[2]. Asad Ullah *et al.*[3] focuses on boundary-layer type Reiner-Philippoff fluid thin film flow. Have investigated the heat transfer and radiation changes caused by the flow of thin Reiner-Philippoff fluid films across a stretching sheet. The time-dependent governing equations for the Reiner-Philippoff fluid model are simplified with the help of similarity variable transformation. The study examined the behavior of the Reiner-Philippoff fluid with a variable stretching surface, considering thermophoresis and Brownian motion characteristics in the flow for

**Author for correspondence*

diverse physical consequences. The increase in flow and heat transfer on a stretching sheet of Reiner-Philippoff nanofluid is described by Gnaneswara Reddy *et al.*[4]. For temperature distributions, the impact of the magnetic field and thermal radiation are investigated. Ganesh Kumar *et al.*[5] applied the Cattaneo-Christov heat diffusion theory to Reiner-Philippoff fluid flow across a hot surface. Ohmic heating, and Cattaneo-Christov heat flux effects are also taken into account. The Reiner-Philippof fuid flow across a stretching sheet is considered by Gnaneswara Reddy *et al.*[6] while taking thermal radiation effect into account. The flow was produced using a linear extending surface with a Darcy-Forchheimer channel applied. Sajid *et al.*[7] examined the effects of distinctive phenomena on non-Newtonian Reiner-Philippoff fluid travelling over a stretchy surface. Muhammad Tahir and Adeel Ahmad[8] examined the effects of fluid pseudoplaticity and dilatancy on non-Newtonian fluid peristaltic flow and heat transfer in a non-uniform asymmetric channel. Ganesh kumar *et al.*[9] studied the thermal effect of the melting heat occurrences for the Reiner-Philippoff fluid flow through stretched Darcy-Forchheimer flow. They noticed that the velocity field is diminished when the Bingham number changes more slowly and thermal field performs better when melting phenomena are present. The energy transit of RPF via a stretched sheet that is inclined vertically is explored by Mallikarjuna *et al.*[10] the flow and heat transmission of Reiner-Philippoff fluid (RPF). They discovered that the fluid velocity is greater for the dilatant fluid and smaller for the pseudo-plastic fluid with higher Bingham number values. For every increase in TB values, the fluid temperature is lower and the fluid velocity is higher.

The free convection nanofluid flow caused by a sheet that is linearly stretched were considered by Makinde and Aziz[11]. The influences of Brownian motion and thermophoresis are accounted for the governing equations. For a sheet with varying thickness, the boundary layers over a continually stretched sheet with a power law surface velocity were addressed by Fang *et al.*[12]. Nadeem *et al.*[13] looked at the Williamson fluid model's two-dimensional flow over a stretching sheet. Numerical analysis is used by Malvandi *et al.*[14] to explore the unsteady double stagnation point flow of a nanofluid across a stretching sheet. Hayat *et al.*[15] investigated is the Maxwell fluid boundary layer flow across a stretching sheet with varying thickness. The Cattaneo-Christov heat flux model is utilised to examine the thermal performance with thermal conductivity variations. The simultaneous Dufour and Soret effects on mass transport and heat in a Casson nanofluid flow over an unstable stretched sheet with heat generation and radiation were explored by Ibukun Sarah Oyelakin *et al.*[16]. Towards a stretching sheet, a mhd flow with magnetic and viscous dissipation effects micropolar nanofluids has been researched by Hsiao[17]. The viscoelastic fluid flow on a stretching sheet is discussed by Ghadikolaei *et al.*[18]. HAM is used to solve the governing equations numerically. The unstable two-dimensional magnetohydrodynamic flow of an incompressible fluid that conducts electricity over a permeable stretched surface in the presence of various slip effects has been designed and simulated by Fazle Mabood and Stanford Shateyi[19]. Under the influence of the first slip, Wubshet Ibrahim and Dachasa Gamachu demonstrated the convection flow of Williamson fluid across an axially stretched surface containing nanoparticles. Punith Gowda *et al.*[20] investigate a unique magnetic dipole influence on ferromagnetic fluid flow across a flat stretchy sheet. Jagadish V. Tawade *et al.*[21] studied the heat transfer of Cassona transverse the linearly stretching sheet to investigate the problem of constant laminar flow of nanofluid on a two-dimensional boundary layer.

2.0 Problem Formulation

The present work investigates the incompressible, laminar, steady-state non-Newtonian fluid flow across a stretched

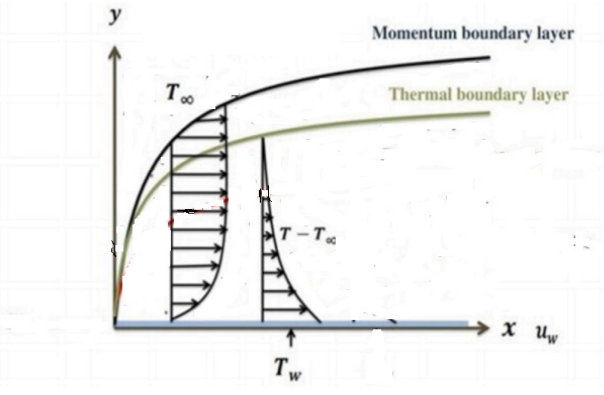

Figure 1. Schematic representation of physical problem.

sheet, as depicted in Figure 1. The y-axis is thought to run parallel to the sheet, and the x-axis is normal to it. Let v and u represent the fluid's velocity in the y- and x-directions. T_w and T_∞ are maintained at and separate from the sheet, respectively.

The governing equations:

$$\frac{\partial u}{\partial x}+\frac{\partial u}{\partial y}=0 \tag{1}$$

$$u\frac{\partial u}{\partial x}+v\frac{\partial u}{\partial y}=\frac{1}{\rho}\left(\frac{\partial T}{\partial x}\right)-\frac{\sigma}{\rho}B_0^{\,2}u \tag{2}$$

$$u\frac{\partial T}{\partial x}+v\frac{\partial T}{\partial y}=\alpha\frac{\partial^2 T}{\partial y^2}+\frac{\mu}{\rho C_p}\left(\frac{\partial u}{\partial y}\right)^2+\frac{\sigma}{\rho C_p}B_0^{\,2}u \tag{3}$$

The boundary constraints:

$$u=ax^{1/2}+S1\frac{\partial u}{\partial y},\ v=0,\ T=T_w \quad \text{at} \quad y=0$$

$$u\to 0,\ T\to T_\infty \quad as \quad y\to\infty \tag{4}$$

Using (4), the equations (1) – (3) become

$$g=\frac{f''\left(g^2+\lambda\Gamma^2\right)}{\Gamma^2+g^2} \tag{5}$$

$$g'=\frac{1}{3}(f')^2-\frac{2}{3}f\,f''-M\,f' \tag{6}$$

$$\theta''+\frac{2}{3}\Pr f\,\theta'+Ec\,(f'')^2+EC\,M\,(f')^2=0 \tag{7}$$

The corresponding dimensionless conditions are:

$$f=0,\ f'=1+a1\,f'',\ \theta=1 \quad \text{as} \quad \eta=0$$

$$f'\to 0,\ \theta\to 0 \ \text{as}\ \eta\to\infty \tag{8}$$

3.0 Numerical Procedure

Analytical solutions to the set of equations (5)–(7) with boundary conditions (8) are challenging. As a result, we employ the shooting technique, one of the best, most straightforward, and precise numerical techniques (Ref. [22] and [23]). The Newton's method, which is not available in (8), is used to determine approximate initial conditions and the fourth order R-K method is used to integrate first order differential equations. Following is. First, by supposing, change higher order equations into first order equations

$$f=f(1)\quad f'=f(2)\quad f''=f(3)\quad \theta=f(4)\quad \theta'=f(5),$$

$$\frac{d}{d\eta}\begin{bmatrix}f(1)\\f(2)\\f(3)\\f(4)\\f(5)\end{bmatrix}=\begin{bmatrix}f(2)\\f(3)\\((g*g+Nu*Nu)/(g*g+lam*Nu*Nu))*((1/3)*f(2)*f(2)-(2/3)*f(3)*f(1)+M*f(2)\\f(5)\\-(2/3)*(Pr)*f(1)*f(5)-Ec*f(3)*f(3)-Ec*M*f(2)*f(2)\end{bmatrix} \tag{9}$$

Eqn. (9) presents a vector form of problem $[f(1)\ f(2)\ f(3)\ f(4)\ f(5)]$ with initial conditions at $f(1)\ f(2)\ f(4)$. The initial conditions that are not stated in eqn. (8) are taken as $f(3)(1)=0.1$, $f(5)(1)=0.2$, and integrate eqn. (9) using Runge Kutta 4th order. Other end circumstances are contrasted with the outcomes that were obtained. Select different initial circumstances and carry out the process again if the difference is greater. It is tiresome to choose the initial conditions at random. To find suitable beginning circumstances, Newton's technique is employed, and RK4 is used to integrate the outcomes.

4.0 Discussion of Results

The impact of various physical limitations on temperature and momentum profiles for several different fluid

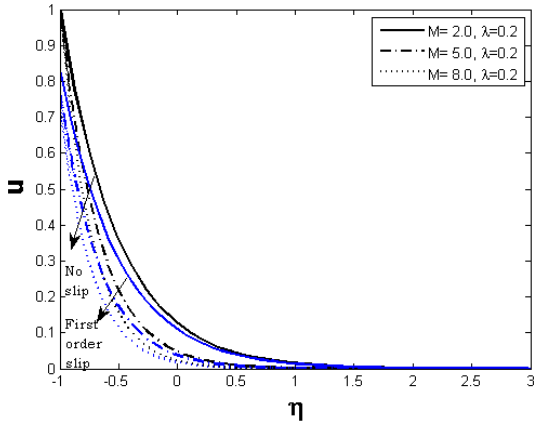

a) For $\lambda=0.2$

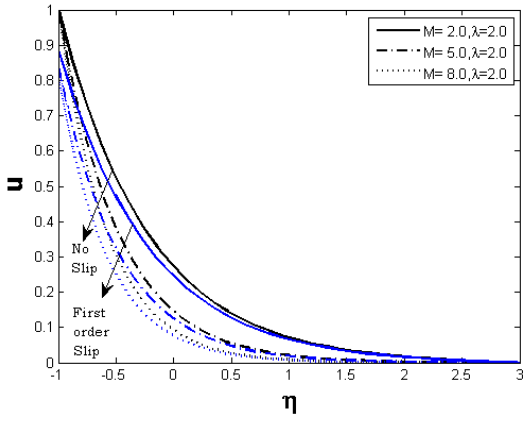

b) For $\lambda=2.0$

Figure 2. Variation of Mon velocity.

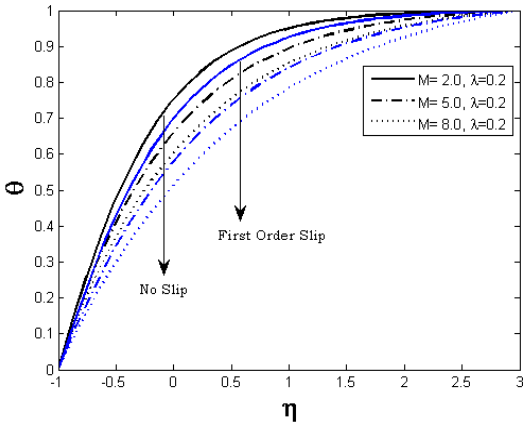

a) For $\lambda = 0.2$

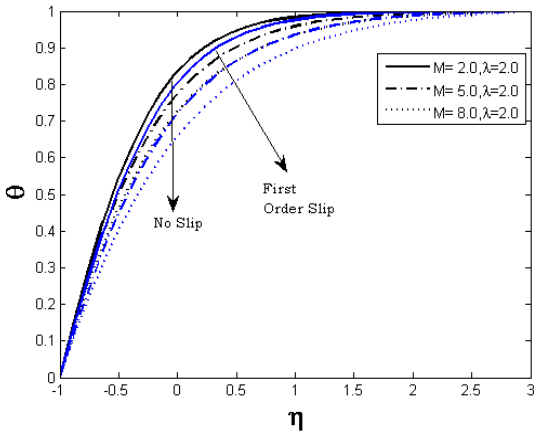

b) For $\lambda = 2.0$

Figure 3. Variation of Mon Temparature.

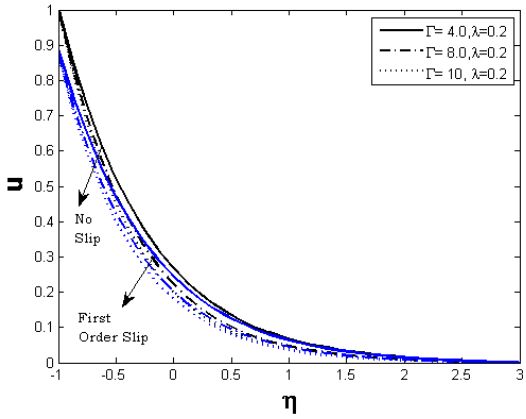

a) For $\lambda = 0.2$

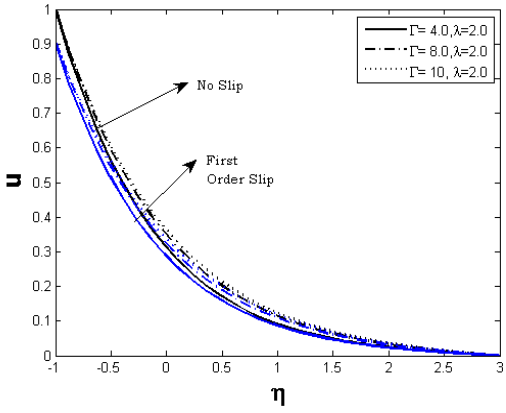

b) For $\lambda = 2.0$

Figure 4. Variation of Γ on Velocity.

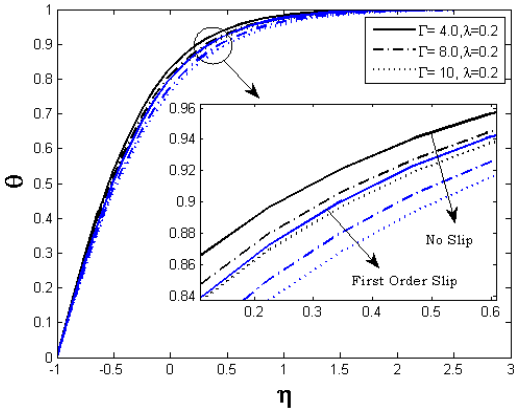

a) For $\lambda = 0.2$

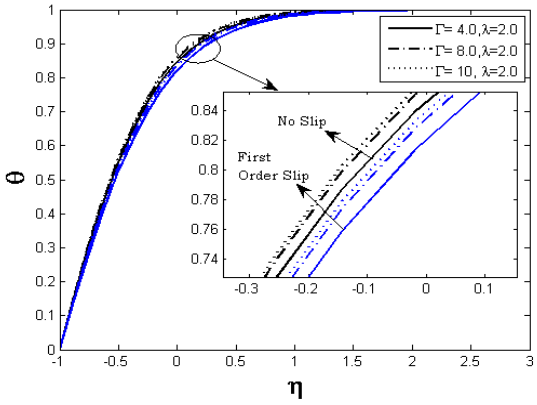

b) For $\lambda = 2.0$

Figure 5. Variation of Γ on Temparature.

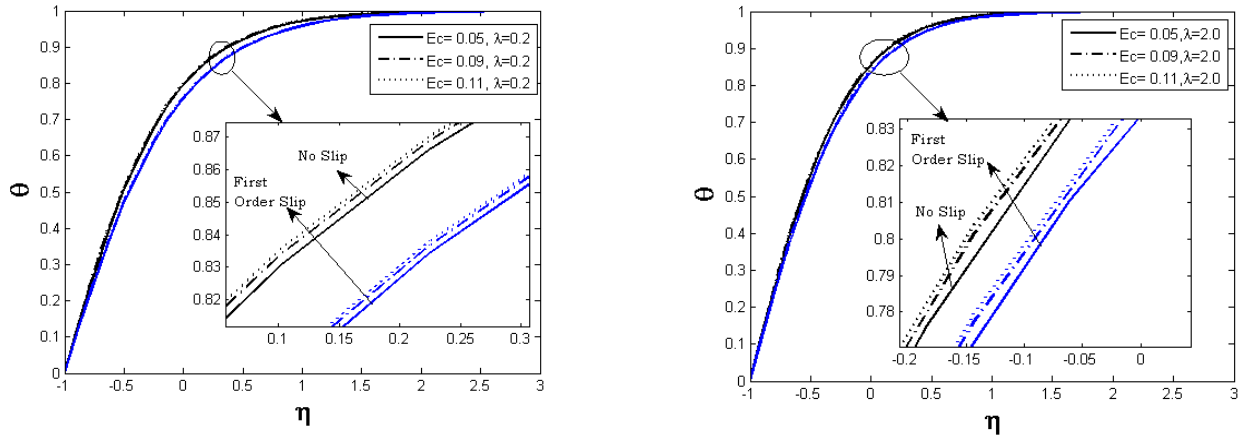

a) For $\lambda = 0.2$ b) For $\lambda = 2.0$

Figure 6. Variation of Ec on Temparature.

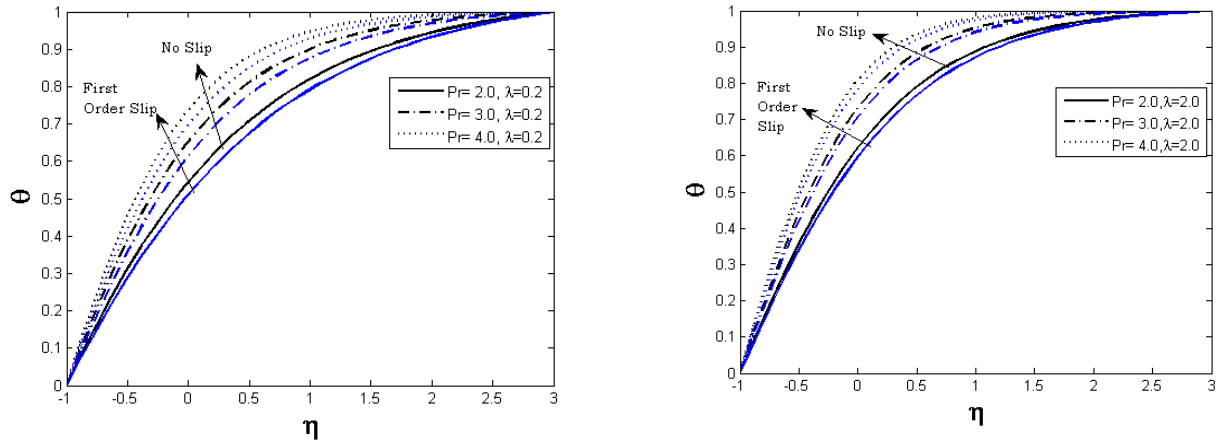

a) For $\lambda = 0.2$ b) For $\lambda = 2.0$

Figure 7. Variation of Pr on Temparature.

Table 1. For a specific Prandtl number, the Nusselt number is obtained for Newtonian fluid flow over a stretching sheet:

Pr	0.7	7.0	10
Patil *et al.*[24]	0.35004	1.38625	1.68011
Chen[25]	0.34925	1.38619	1.68008
Mallikarjuna *et al.*[24]	0.3488	1.3863	1.6802
Present	0.34892	1.38651	1.68032

scenarios is reported and assessed in this section (Table 2), including Magnetic parameter, Eckert number, Bingham number. Unless otherwise stated, the physical parameters are assumed to have default values of Magnetic parameter M = 2, Eckert number Ec= 0.1, Bingham number Γ = 2.0 and Prandtl number Pr = 5.

Table 2. Three different cases of the fluids

Case 1	$\lambda < 1$	Dilatant fluid
Case 2	$\lambda = 1$	Newtonian fluid
Case 3	$\lambda > 1$	Pseudo plastic fluid

Numerical values for Nusselt number:

Table 3. For $\lambda = 0.2$

No Slip					
M	**Γ**	**Ec**	**Pr**	**a1**	**Nu**
1	2	0.1	5	0.0	-1.2637
2					-1.2238
3					-1.1939
4					-1.1707
	2				-1.2637
	5				-1.2464
	6				-1.2384
	8				-1.2206
		0.1			-1.2637
		0.2			-1.3417
		0.3			-1.4196
		0.4			-1.4976
			1		-0.5419
			3		-0.9426
			4		-1.1122
			5		-1.2637

First Order Slip					
M	Γ	Ec	Pr	a1	Nu
1	2	0.1	5	0.5	-0.9402
2					-0.8136
3					-0.7268
4					-0.6641
	2				-0.9402
	5				-0.9079
	6				-0.8932
	8				-0.8611
		0.1			-0.9402
		0.2			-0.9726
		0.3			-1.0049
		0.4			-1.0373
			1		-0.4159
			3		-0.6930
			4		-0.8217
			5		-0.9402

The effect of M on fluid velocity is depicted in Figure 2. For $\lambda = 0.2,\ 2.0$, the fluid velocity decreases as M values increase in both the zero slip and first slip scenarios. Figure 3 shows how M affects the temperature of the fluid. The fluid temperature drops as M values rise for lam = 0.2, 2.0 in both the zero slip and first slip cases. The effect of the Γ on the velocity profile for three distinct RPF parameter instances is shown in Figure 4. Because of the low viscosity caused by a higher shear rate, the yield stress or the viscous stress both decrease as the rise, slowing the flow rate for the dilatant fluid. Consequently, dilatant fluid flow thickens. It is significant to remember that, as fluid velocity increases, the dilatant fluid decreases (Figure 4a). Pseudo plastic fluid exhibits the exact opposite behaviour from Figure 4b for the both cases of zero slip and first slip. Figure 5 illustrates how fluid temperature affects. It has been noted that as the Bingham number increases, the dilatant fluid's temperature rises. However, the flow of pseudoplastic fluid shows a reversal pattern for the case of zero slip and first slip. The influence of Ec on

Table 4. For $\lambda = 2.0$

No Slip					
M	**Γ**	**Ec**	**Pr**	**a1**	**Nu**
1	2	0.1	5	0.0	-1.2717
2					-1.2340
3					-1.2056
4					-1.1834
	2				-1.2717
	5				-1.2878
	6				-1.2934
	8				-1.3032
		0.1			-1.2717
		0.2			-1.3484
		0.3			-1.4250
		0.4			-1.5017
			1		-0.5452
			3		-0.9501
			4		-1.1201
			5		-1.2717

First Order Slip					
M	Γ	Ec	Pr	a1	Nu
1	2	0.1	5	0.5	-0.9554
2					-0.8311
3					-0.7448
4					-0.6815
	2				-0.9554
	5				-0.9863
	6				-0.9972
	8				-1.0164
		0.1			-0.9554
		0.2			-0.9880
		0.3			-1.0207
		0.4			-1.0533
			1		-0.4207
			3		-0.7049
			4		-0.8356
			5		-0.9554

temperature profile is shown in Figure 6. The fluid temperature will go up for lam = 0.2, 2.0 for the instances of zero slip as well as the first slip with greater values of Ec. Figure 7 depicts how the Pr affects the temperature profile. For lam = 0.2, 2.0 for occurrences of zero slip as well as the first slip with higher values of Pr, the fluid temperature will rise.

Nusslet number values for various λ values are shown in Tables 3 and 4. Table 3 shows that for the situations of λ =0.2, the heat transfer coefficient grows for M, Γ and falls for Ec, Pr for both nil slip as well as first slip. According to Table 4, for cases where lam = 2.0, the heat transfer coefficient improves for M and drops for Γ, Ec, Pr for both nil slip and first slip.

5.0 Conclusion

In the current work, the energy transit of RPF past a stretched sheet is explored and reported. By using RK4, the modelled expressions are numerically solved. Visual representations of velocity and temperature profiles under various scenarios include the Magnetic parameter, Bingham number, Eckert number, and Prandtl number. Our findings are:

- With greater values of for both the first slip and nil slip scenarios, the fluid velocity is higher in the pseudo-plastic fluid scenario and lower in the dilatant fluid scenario.
- For all case studies of λ, a boost in M caused a decrease in fluid velocity and temperature for nil slip and first slip.
- Γ, Ec, and Pr see a decline in the Nusselt number for pseudo-plastic fluid.

6.0 References

1. Gupta RC. Two-dimensional flow of Reiner-Philippoff fluids in the inlet length of a straight channel. (n.d.).

2. Ahmad A. Flow of Reiner-Philippoff based nano-fluid past a stretching sheet. J Mol Liq. 2016; 219:643–646. https://doi.org/10.1016/j.molliq.2016.03.068.
3. Ullah A, Alzahrani EO, Shah Z, Ayaz M, Islam S. Nanofluids thin film flow of Reiner-Philippoff fluid over an unstable stretching surface with Brownian motion and thermophoresis effects. Coatings. 2019. https://doi.org/10.3390/coatings9010021.
4. Reddy MG, Rani S, Kumar KG, Seikh AH, Rahimi-Gorji M, Sherif ESM. Transverse magnetic flow over a Reiner-Philippoff nanofluid by considering solar radiation. Mod Phys Lett B. 2019; 33:1–15. https://doi.org/10.1142/S0217984919504499.
5. Kumar KG, Reddy MG, Sudharani MVVL, Shehzad SA, Chamkha AJ. Cattaneo–Christov heat diffusion phenomenon in Reiner–Philippoff fluid through a transverse magnetic field. Phys A Stat Mech Its Appl. 2020. https://doi.org/10.1016/j.physa.2019.123330.
6. Reddy MG, Sudharani MVVL, Kumar GK, Chamkha AJ, Lorenzini G. Physical aspects of Darcy–Forchheimer flow and dissipative heat transfer of Reiner–Philippoff fluid. J Therm Anal Calorim. 2020; 141:829–838. https://doi.org/10.1007/s10973-019-09072-0.
7. Sajid T, Sagheer M, Hussain S. Impact of Temperature-Dependent Heat Source/Sink and Variable Species Diffusivity on Radiative Reiner-Philippoff Fluid. Math Probl Eng. 2020. https://doi.org/10.1155/2020/9701860.
8. Tahir M, Ahmad A. Impact of pseudoplaticity and dilatancy of fluid on peristaltic flow and heat transfer: Reiner-Philippoff fluid model. Adv Mech Eng. 2020; 12:1–10. https://doi.org/10.1177/1687814020981184.
9. Kumar GK, Reddy MG, Khan MI, Alzahrani F, Khan MI, El-Zahar ER. Heat transfer and melting flow of a Reiner-Philippoff fluid over a surface with Darcy-Forchheimer medium. Case Stud Therm Eng. 2021; 28:101649. https://doi.org/10.1016/j.csite.2021.101649.
10. Mallikarjuna B, Chakravarthy YSK, Raju CSK, Ayyaz R, Shehzad SA. Spectral-quasi-linearization method and multiple regression analysis of Reiner-Philippoff fluid flow. ZAMM Zeitschrift Fur Angew Math Und Mech. 2022. https://doi.org/10.1002/zamm.202100071.
11. Makinde OD, Aziz A. Boundary layer flow of a nanofluid past a stretching sheet with a convective boundary condition. Int J Therm Sci. 2011; 50:1326–1332. https://doi.org/10.1016/j.ijthermalsci.2011.02.019.
12. Fang T, Zhang J, Zhong Y. Boundary layer flow over a stretching sheet with variable thickness. Appl Math Comput. 2012; 218:7241–7252. https://doi.org/10.1016/j.amc.2011.12.094.
13. Nadeem S, Hussain ST, Lee C. Flow of a Williamson fluid over a stretching sheet. Braz J Chem Eng. 2013; 30:619–625. https://doi.org/10.1590/S0104-66322013000300019.
14. Malvandi A, Hedayati F, Ganji DD. Slip effects on unsteady stagnation point flow of a nanofluid over a stretching sheet. Powder Technol. 2014; 253:377–384. https://doi.org/10.1016/j.powtec.2013.11.049.
15. Hayat T, Farooq M, Alsaedi A, Al-Solamy F. Impact of Cattaneo-Christov heat flux in the flow over a stretching sheet with variable thickness. AIP Adv. 2015; 5:0–12. https://doi.org/10.1063/1.4929523.
16. Oyelakin IS, Mondal S, Sibanda P. Unsteady Casson nanofluid flow over a stretching sheet with thermal radiation, convective and slip boundary conditions. Alexandria Eng J. 2016; 55:1025–1035. https://doi.org/10.1016/j.aej.2016.03.003.
17. Hsiao KL. Micropolar nanofluid flow with MHD and viscous dissipation effects towards a stretching sheet with multimedia feature. Int J Heat Mass Transf. 2017; 112:983–990. https://doi.org/10.1016/j.ijheatmasstransfer.2017.05.042.
18. Ghadikolaei SS, Hosseinzadeh K, Yassari M, Sadeghi H, Ganji DD. Analytical and numerical solution of non-Newtonian second-grade fluid flow on a stretching sheet. Therm Sci Eng Prog. 2018; 5:309–316. https://doi.org/10.1016/j.tsep.2017.12.010.
19. Mabood F, Shateyi S. Multiple Slip Effects on MHD Unsteady Flow Heat and Mass Transfer Impinging on Permeable Stretching Sheet with Radiation. Model Simul Eng. 2019. https://doi.org/10.1155/2019/3052790.
20. Punith Gowda RJ, Naveen Kumar R, Prasannakumara BC, Nagaraja B, Gireesha BJ. Exploring magnetic dipole contribution on ferromagnetic nanofluid flow over a stretching sheet: An application of Stefan blowing. J Mol Liq. 2021; 335:116215. https://doi.org/10.1016/j.molliq.2021.116215.
21. Tawade JV, Guled CN, Noeiaghdam S, Fernandez-Gamiz U, Govindan V, Balamuralitharan S. Effects of thermophoresis and Brownian motion for thermal and chemically reacting Casson nanofluid flow over a linearly stretching sheet. Results Eng. 2022; 15:100448. https://doi.org/10.1016/j.rineng.2022.100448.
22. Raza J, Rohni AM, Omar Z, MHD flow and heat transfer of Cu–water nanofluid in a semi-porous channel with stretching walls. Int J Heat Mass Transf. 2016;

103:336–340. https://doi.org/10.1016/j.ijheatmasstransfer.2016.07.064.
23. Rashad AM, Mallikarjuna B, Chamkha AJ, Raju SH. Thermophoresis effect on heat and mass transfer from a rotating cone in a porous medium with thermal radiation. Afrika Mat. 2016; 27:1409–1424. https://doi.org/10.1007/s13370-016-0421-4.
24. Patil PM, Roy S, Chamkha AJ. Mixed convection flow over a vertical power-law stretching sheet. Int J Numer Methods Heat Fluid Flow. 2010; 20:445–458. https://doi.org/10.1108/09615531011035839.
25. Chen CH. Laminar mixed convection adjacent to vertical, continuously stretching sheets. Heat Mass Transf. Und Stoffuebertragung. 1998; 33:471–476. https://doi.org/10.1007/s002310050217.